

Aggregate dust model to study the polarization properties of comet C/1996 B2 Hyakutake

Himadri Sekhar Das, Abinash Suklabaidya, Saonli Datta Majumder and Asoke Kumar Sen

Department of Physics, Assam University, Silchar 788011, India; hsdas@iucaa.ernet.in

Received 2009 July 31; accepted 2010 January 4

Abstract The observed linear polarization data of comet Hyakutake are studied at wavelengths $\lambda = 0.365 \mu\text{m}$, $\lambda = 0.485 \mu\text{m}$ and $0.684 \mu\text{m}$ through simulations using Ballistic Particle-Cluster Aggregate and Ballistic Cluster-Cluster Aggregate aggregates of 128 spherical monomers. We first found that the size parameter of the monomer, $x \sim 1.56 - 1.70$, turned out to be the most suitable which provides the best fits to the observed dust scattering properties at three wavelengths: $\lambda = 0.365 \mu\text{m}$, $0.485 \mu\text{m}$ and $0.684 \mu\text{m}$. Thus, the effective radius of the aggregate (r) lies in the range $0.45 \mu\text{m} \leq r \leq 0.49 \mu\text{m}$ at $\lambda = 0.365 \mu\text{m}$; $0.60 \mu\text{m} \leq r \leq 0.66 \mu\text{m}$ at $\lambda = 0.485 \mu\text{m}$ and $0.88 \mu\text{m} \leq r \leq 0.94 \mu\text{m}$ at $\lambda = 0.684 \mu\text{m}$. Now using superposition T-MATRIX code and the power-law size distribution, $n(r) \sim r^{-3}$, the best-fitting values of complex refractive indices are calculated for the observed polarization data at the above three wavelengths. The best-fitting complex refractive indices (n, k) are found to be (1.745, 0.095) at $\lambda = 0.365 \mu\text{m}$, (1.743, 0.100) at $\lambda = 0.485 \mu\text{m}$ and (1.695, 0.100) at $\lambda = 0.684 \mu\text{m}$. The refractive indices derived from the present analysis correspond to a mixture of both silicates and organics, which are in good agreement with the *in situ* measurement of comets by different spacecraft.

Key words: comets: general — dust, extinction — scattering — polarization

1 INTRODUCTION

The study of cometary polarization, over various scattering angles and wavelengths, gives valuable information about the nature of cometary dust. The numerical and experimental simulations of polarization data give information about the physical properties of the cometary dust, which include size distribution, shape and complex refractive indices. Several investigators (Kikuchi et al. 1987; Lamy et al. 1987; Sen et al. 1991a,b; Chernova et al. 1993; Xing & Hanner 1997; Petrova et al. 2004; Kimura et al. 2006; Das et al. 2004; Kolokolova et al. 2007; Bertini et al. 2007 etc.) have studied linear and circular polarization measurements of many comets. These studies help us to understand the dust grain nature of comets.

Comet Hyakutake (C/1996 B2) was the brightest comet to appear in the sky in the year 1996. Its passage near the Earth was one of the closest cometary approaches in the previous 200 years. The comet passed within 0.1 AU of the Earth in March 1996. Comet Hyakutake was bright enough to make high precision polarimetric observations during its pre-perihelion phase. Observations of the linear polarization of comet Hyakutake were carried out at three different wavelengths: $0.365 \mu\text{m}$, $0.485 \mu\text{m}$ and $0.684 \mu\text{m}$ by different investigators (Joshi et al. 1997; Kiselev & Velichko 1998 and Manset & Bastien 2000).

Greenberg & Hage (1990) first suggested that cometary particles are not spherical and porous. They originally proposed the presence of large numbers of *porous* grains in the coma of comets to explain the spectral emission at $3.4 \mu\text{m}$ and $9.7 \mu\text{m}$. Dollfus (1989) discussed the results of laboratory experiments by microwave simulation and laser scattering on various complex shapes with different porosities. The results of *in situ* measurements carried out on the Giotto spacecraft of Comet Halley (Fulle et al. 2000) and the analysis of the infrared spectra of Comet Hale-Bopp (Moreno et al. 2003) also agree with the model of aggregates. It is clear from the recent modeling of optical observations (Xing & Hanner 1997; Kimura 2001; Kimura et al. 2006; Petrova et al. 2004; Tishkovets et al. 2004; Lasue & Levasseur-Regourd 2006; Kolokolova et al. 2007; Bertini et al. 2007; Levasseur-Regourd et al. 2007, 2008; Das et al. 2008a,b etc.), thermal-infrared observations (Lisse et al. 1998; Harker et al. 2002), laboratory studies (Wurm & Blum 1998; Gustafson & Kolokolova 1999; Hadamcik et al. 2002 etc.), and especially from the ‘Stardust’ returned samples (Hörz et al. 2006), that cometary dust consists of irregular, mostly aggregated particles.

Das & Sen (2006) studied the non-spherical dust grain characteristics of Comet Levy 1990XX using T-matrix theory. They found that compact prolate grains as compared to spherical grains can better explain the observed linear polarization data. Recently, Das et al. (2008a) have again analyzed the observed polarization data of Comet Levy 1990XX and successfully reproduced the polarization curve through simulations using an aggregate dust model, where the fit was even better. It has been found from their analysis that aggregate particles can produce an even better fit to the observed data as compared to compact prolate grains. Recently, using an aggregate dust model, Das et al. (2008b) successfully explained the polarization characteristics of comet Hale-Bopp at $\lambda = 0.485 \mu\text{m}$ and $0.684 \mu\text{m}$. Lasue et al. (2009) have successfully explained the polarization properties of comets Hale-Bopp and Halley by using a model of light scattering through a size distribution of aggregates (spherical or spheroidal) mixed with single spheroidal particles.

In the present work, the aggregate dust model is proposed for studying the observed polarization data of Comet Hyakutake at $\lambda = 0.365 \mu\text{m}$, $0.485 \mu\text{m}$ and $0.684 \mu\text{m}$.

2 AGGREGATE MODEL OF COMETARY DUST

The aggregates are built by using ballistic aggregation procedures. Two types of aggregates are considered here-BPCA (Ballistic Particle-Cluster Aggregate) and BCCA (Ballistic Cluster-Cluster Aggregate). In the actual case, the BPCA clusters are more compact than BCCA clusters (Mukai et al. 1992). A systematic explanation of the dust aggregate model was already discussed in our previous work (Das et al. 2008a). Laboratory diagnosis of particle coagulation in the solar nebula suggests that the particles grow under the BCCA process. It is also found that the morphology of dust particles does not play a major role in determining the shape of polarization (Kimura 2001; Kimura et al. 2003, 2006; Kolokolova et al. 2006; Lasue & Levasseur-Regourd 2006; Bertini et al. 2007; Das et al. 2008a,b). The size of the individual monomer in a cluster plays an important role in scattering calculations. These have been confirmed by the results of previous work on the dust aggregate model (Kimura et al. 2003; Kimura et al. 2006; Petrova et al. 2004; Hadamcik et al. 2006; Bertini et al. 2007) and also from our previous work (Das et al. 2008a).

3 COMPOSITION

The *in situ* observations of comets, laboratory analysis of samples of Interplanetary Dust Particles (IDP) and remote infrared spectroscopic studies of comets give useful information about the composition of cometary dust. The *in situ* measurement of impact-ionization mass spectra of Comet Halley’s dust has suggested that the dust consists of magnesium-rich silicates, carbonaceous materials, and iron-bearing sulfides (Kissel et al. 1986; Jessberger et al. 1988; Jessberger 1999). Actually, the first evidence for carbonaceous material in comets comes from the study of Vega spacecraft data by Kissel et al. (1986). These materials are also known to be the major constituents of IDPs

(Brownlee et al. 1980). The studies of comets and IDPs have shown the presence of amorphous and crystalline silicate minerals (e.g. forsterite, enstatite) and organic materials (Hanner & Bradley 2004). Laboratory studies have shown that the majority of the collected IDPs fall into the spectral classes defined by their $10\ \mu\text{m}$ feature profiles. These observed profiles indicate the presence of pyroxene, olivine and layer lattice silicates. This is in good agreement with results obtained from Giotto and Vega mass spectrometer observations of Comet Halley (Lamy et al. 1987). The infrared (IR) measurement of comets has also provided important information on the silicate compositions in cometary dust. The spectroscopic studies of silicates have shown the predominance of both crystalline and amorphous silicates consisting of pyroxene or olivine grains (Wooden et al. 1999; Hayward et al. 2000; Bockelée - Morvan et al. 2002 etc.). Mg-rich crystals are also found within IDPs and are predicted by comparing the IR spectral features of Comet Hale-Bopp with synthetic spectra obtained from laboratory studies (Hanner 1999; Wooden et al. 1999, 2000). ‘Stardust’ samples have also confirmed a variety of olivine and pyroxene silicates in Comet 81P/Wild 2 (Zolensky et al. 2006).

Levasseur-Regourd et al. (1996) studied a polarimetric database of several comets and from the nature of the phase angle (α) dependence, they concluded that there is clear evidence for at least two classes of comets according to the values of polarization at $\alpha \approx 80^\circ - 100^\circ$: comets with a high maximum in polarization, of about 25% for one group and smaller than 15% for the other group. The two classes of comets are distinct only for $\alpha > 35^\circ$. It has also been observed that there is a very good correlation between the existence of a high maximum in polarization and a strong silicate emission feature (Levasseur-Regourd 1999). The observed polarization data of comet Hyakutake showed a high maximum in polarization. The polarization at a given phase angle larger than 30° most often increases linearly with increasing wavelength in the visible domain and this increase is steeper for larger phase angles (Levasseur-Regourd & Hadamcik 2003). Recent studies have provided useful information about the two groups of polarimetrically different comets (Kiselev et al. 2001; Kiselev et al. 2004; Jewitt 2004; Jockers et al. 2005).

It has already been found that the silicate composition can best reproduce the observed polarization data of Comet Levy 1990XX and Comet Hale-Bopp (Das et al. 2008a,b).

4 NUMERICAL SIMULATIONS

The scattering calculations for BCCA & BPCA particles have been done by the Superposition T-matrix code, which gives rigorous solutions for ensembles of spheres (Mackowski & Mishchenko 1996). The observed linear polarization data of comet Hyakutake at $\lambda = 0.365\ \mu\text{m}$, $0.485\ \mu\text{m}$ and $0.684\ \mu\text{m}$ are taken from Joshi et al. (1997), Kiselev & Velichko (1998) and Manset & Bastien (2000).

The linear polarization is given by

$$P(\theta) = -\frac{S_{21}}{S_{11}}. \quad (1)$$

For modeling comet Hyakutake, we will use a power-law size distribution, $n(r) = dn/dr \sim r^{-3}$. For a particular type of aggregate with fixed N , the size distribution is just $dn/da_m \sim a_m^{-3}$. Thus, the averaged polarization is (Shen et al. 2009):

$$\bar{P} = \frac{\int_{a_{\min}}^{a_{\max}} p(a_m, \theta) S_{11}(a_m, \theta) n(a_m) da_m}{\int_{a_{\min}}^{a_{\max}} S_{11}(a_m, \theta) n(a_m) da_m}, \quad (2)$$

where a_{\min} and a_{\max} are the minimum and maximum values of the monomer size in our size distribution.

The radius of an aggregate particle can be described by the radius of a sphere of equal volume given by $r = a_m N^{1/3}$, where N is the number of monomers in the aggregate. In the present work,

$N = 128$ is taken. The size parameter of the monomer is given by $x = \frac{2\pi a_m}{\lambda}$. We first found that $x \sim 1.56 - 1.70$ turned out to be the most suitable parameter that provides the best qualitative fits to the observed dust scattering properties at three wavelengths: $\lambda = 0.365 \mu\text{m}$, $0.485 \mu\text{m}$ and $0.684 \mu\text{m}$. This corresponds to $0.090 \mu\text{m} \leq a_m \leq 0.098 \mu\text{m}$ at $\lambda = 0.365 \mu\text{m}$, $0.120 \mu\text{m} \leq a_m \leq 0.131 \mu\text{m}$ at $\lambda = 0.485 \mu\text{m}$ and $0.174 \mu\text{m} \leq a_m \leq 0.186 \mu\text{m}$ at $\lambda = 0.684 \mu\text{m}$. Thus, the effective radius of the aggregate (r) lies in the range $0.45 \mu\text{m} \leq r \leq 0.49 \mu\text{m}$ at $\lambda = 0.365 \mu\text{m}$, $0.60 \mu\text{m} \leq r \leq 0.66 \mu\text{m}$ at $\lambda = 0.485 \mu\text{m}$ and $0.88 \mu\text{m} \leq r \leq 0.94 \mu\text{m}$ at $\lambda = 0.684 \mu\text{m}$.

We start calculations considering the refractive indices of amorphous pyroxene and amorphous olivine at $\lambda = 0.365 \mu\text{m}$, $0.485 \mu\text{m}$ and $0.684 \mu\text{m}$. The refractive indices of the materials are calculated by linearly interpolating the data obtained from laboratory studies (Dorschner et al. 1995). Olivines and pyroxenes are described by $\text{Mg}_{2y}\text{Fe}_{2-2y}\text{SiO}_4$, with $y = 0.4$, and 0.5 ; and $\text{Mg}_y\text{Fe}_{1-y}\text{SiO}_3$, with $y = 1.00, 0.95, 0.8, 0.7, 0.6, 0.5$ and 0.4 .

It has already been investigated that the choice of the above values of refractive indices cannot match the observed polarization data of Comet Levy 1990XX and Comet Hale-Bopp (Das et al. 2008a,b). The same set of refractive indices is now chosen to fit the observed polarization data of Comet Hyakutake. The calculations have been done for BCCA aggregates. However, no such good fit has been observed using the above values of refractive indices. Next, the calculation has been repeated for carbonaceous materials, but none of them could match the observed data well.

We now use the χ^2 minimization technique to evaluate the best-fitting values of (n, k) which can fit the observed polarization data. We have already used this minimization technique to fit the observed linear polarization data of Comet Levy 1990XX at $\lambda = 0.485 \mu\text{m}$ and Comet Hale-Bopp at $\lambda = 0.485 \mu\text{m}$ and $0.684 \mu\text{m}$ (Das et al. 2008a,b) with aggregate models of dust.

The error in the fitting procedure can be defined as

$$\chi_{\text{pol}}^2 = \sum_{i=1}^J \left| \frac{P_{\text{obs}}(\theta_i, \lambda) - P_{\text{model}}(\theta_i, \lambda)}{E_p(\theta_i, \lambda)} \right|^2, \quad (3)$$

where $P_{\text{obs}}(\theta_i, \lambda)$ is the degree of observed linear polarization at scattering angle θ_i ($i = 1, 2, \dots, J$) and wavelength λ , $P_{\text{model}}(\theta_i, \lambda)$ is the polarization values obtained from model calculations and $E_p(\theta_i, \lambda)$ is the error in the observed polarization at scattering angle θ_i and wavelength (λ).

We now introduce a quantity $\chi^2 = \chi_{\text{pol}}^2 / J$, where J is the number of data points. The values of (n, k) vary over a large range simultaneously with a_m and we find for a particular value of (n, k) , χ^2 reaches a minimum. This particular value of (n, k) is our best fitted (n, k) value and the corresponding minimum value of χ^2 is denoted as χ_{min}^2 . It is also observed that this technique of minimization of χ^2 is quite unique. The value of χ_{min}^2 gives the confidence level on our best fit values of (n, k) and also in the overall fitting procedure.

We need to fine-tune the free parameters (n, k) in the model to make the best fit to the observed linear polarization data of Comet Hyakutake. The real part of the refractive index increases from $n = 1.4$ to 2.0 in steps of 0.001 , while the imaginary part of the refractive index increases from $k = 0.001$ to 1.0 in steps of 0.001 . The same range has already been used for Comet Levy 1990XX and Comet Hale-Bopp (Das et al. 2008a,b).

Now, we analyze the observed data of comet Hyakutake at $0.365 \mu\text{m}$. We calculate \bar{P} averaged over the size distribution $n(r) \sim r^{-3}$ with $r_{\text{min}} = 0.45 \mu\text{m}$ and $r_{\text{max}} = 0.49 \mu\text{m}$ ($a_{\text{min}} = 0.090 \mu\text{m}$, $a_{\text{max}} = 0.098 \mu\text{m}$). The best fitting refractive index at $0.365 \mu\text{m}$ is found to be $n = 1.745$, and $k = 0.095$. The simulated polarization curve at $0.365 \mu\text{m}$ is shown in Figure 1.

We now extend our calculation further to fit the observed polarization data at $\lambda = 0.485 \mu\text{m}$ and $0.684 \mu\text{m}$. Here, we also calculate \bar{P} averaged over the size distribution $n(r) \sim r^{-3}$ with $r_{\text{min}} = 0.60 \mu\text{m}$ and $r_{\text{max}} = 0.66 \mu\text{m}$ ($a_{\text{min}} = 0.120 \mu\text{m}$, $a_{\text{max}} = 0.131 \mu\text{m}$) at $\lambda = 0.485 \mu\text{m}$, and $r_{\text{min}} = 0.88 \mu\text{m}$ and $r_{\text{max}} = 0.94 \mu\text{m}$ ($a_{\text{min}} = 0.174 \mu\text{m}$, $a_{\text{max}} = 0.186 \mu\text{m}$) at $\lambda = 0.684 \mu\text{m}$. The

best fitting refractive indices obtained from the present analysis are found to be (1.743, 0.100) at $\lambda = 0.485 \mu\text{m}$ and (1.695, 0.100) at $\lambda = 0.684 \mu\text{m}$. The simulated polarization curves for comet Hyakutake at $\lambda = 0.485 \mu\text{m}$ and $0.684 \mu\text{m}$ for BCCA aggregates are shown in Figures 2 and 3.

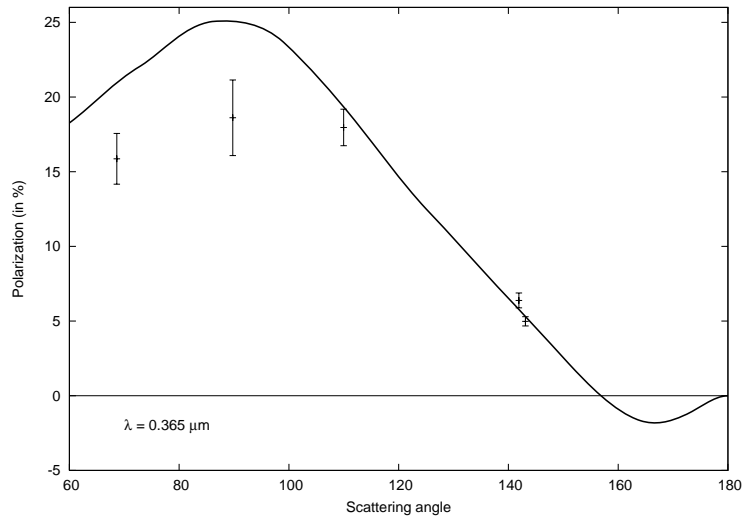


Fig. 1 Polarization values as observed at wavelength $\lambda = 0.365 \mu\text{m}$ for comet Hyakutake by Joshi et al. (1997) and Kiselev & Velichko (1998). The solid curve represents the best-fitting polarization curve obtained for BCCA particles with 128 monomers for a size distribution $n(r) \sim r^{-3}$ for $0.45 \mu\text{m} \leq r \leq 0.49 \mu\text{m}$ at $\lambda = 0.365 \mu\text{m}$. Here, $n = 1.745$ and $k = 0.095$.

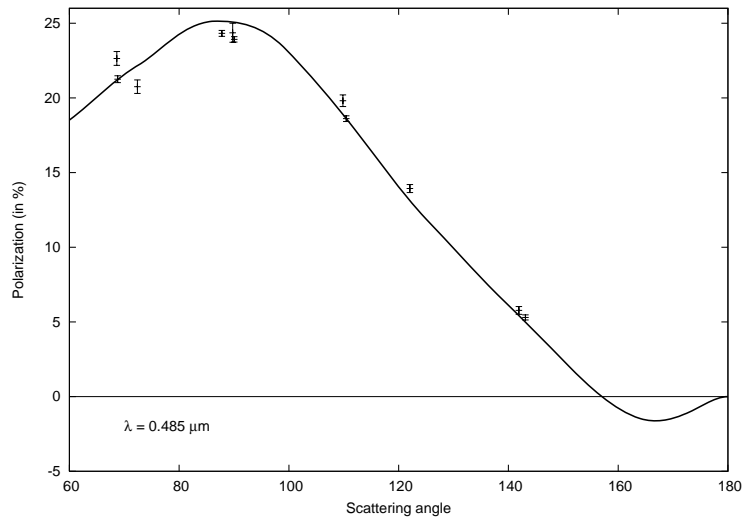


Fig. 2 Polarization values as observed at wavelength $\lambda = 0.485 \mu\text{m}$ for comet Hyakutake by Joshi et al. (1997) and Kiselev & Velichko (1998). The solid curve represents the best-fitting polarization curve obtained for BCCA particles with 128 monomers for a size distribution $n(r) \sim r^{-3}$ for $0.60 \mu\text{m} \leq r \leq 0.66 \mu\text{m}$ at $\lambda = 0.485 \mu\text{m}$. Here, $n = 1.743$ and $k = 0.100$.

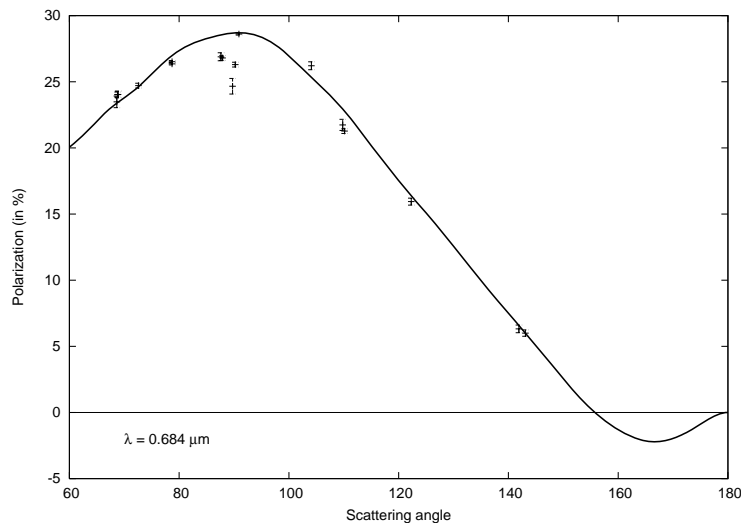


Fig. 3 Polarization values as observed at wavelength $\lambda = 0.684 \mu\text{m}$ for comet Hyakutake by Joshi et al. (1997), Kiselev & Velichko (1998) and Manset & Bastien (2000). The solid curve represents the best-fitting polarization curve obtained for BCCA particles with 128 monomers for a size distribution $n(r) \sim r^{-3}$ for $0.88 \mu\text{m} \leq r \leq 0.94 \mu\text{m}$ at $\lambda = 0.684 \mu\text{m}$. Here, $n = 1.695$ and $k = 0.100$.

5 DISCUSSION

The negative polarization behavior of a comet is one of the major features observed in comets. Several comets show negative polarization beyond the 157° scattering angle (Kikuchi et al. 1987; Chernova et al. 1993; Ganesh et al. 1998, etc.). Interestingly, all comets show very similar characteristics of negative polarization (minimum value of polarization $\sim -2\%$ near 170° and inversion angle at $20^\circ - 22^\circ$). Comet Hyakutake was observed over a wide scattering angle range ($68.6^\circ - 143.1^\circ$), but there was no observation recorded beyond 143.1° (Joshi et al. 1997; Kiselev & Velichko 1998 and Manset & Bastien 2000). In the present work, it is interesting to observe that the dust aggregate model which we used reproduces the negative polarization behavior beyond 157° .

The strength of the silicate feature is defined as the ratio of the flux between 10 and $11 \mu\text{m}$ to that of the underlying continuum (Lisse 2002; Sitko et al. 2004; Kolokolova et al. 2007). The silicate feature strength of Comet Hyakutake is > 1.5 (Lisse 2002) whereas the values for Comet Levy 1990XX and Comet Hale-Bopp are given by 1.8 (Harker et al. 1999) and 2.16 (Sitko et al. 2004), respectively. Comet Hale-Bopp is an intrinsically bright comet, with polarization values much higher than those of other comets. It has been found that Comet Hale-Bopp shows the highest silicate feature strength. The strong silicate feature indicates a high abundance of silicates in the dust. It can be seen that the refractive indices coming out from the present calculation is close to the refractive indices of silicates and organics. Again, the *in situ* measurements of comet Halley (Lamy et al. 1987) and the ‘Stardust’ returned samples of comet Wild 2 (Zolensky et al. 2006) showed the presence of a mixture of silicates and organic refractory in the cometary dust. Thus, our model calculations represent the more realistic type of grains which may be considered as a mixture of silicates and carbonaceous materials. It should be noted that the presence of negative polarization in the backscatter domain has been commonly attributed to silicates or dirty ice grains (Kimura et al. 2006).

It has been investigated that the aggregate dust model can fit the observed polarization data of comet Hyakutake well when the size parameter of the monomer $x \sim 1.56-1.70$. Thus, the size

ranges of the monomer differ for three wavelengths, which is unlikely. The proposed model can be further developed if we take a mixture of compact spheroidal grains and aggregates over a wide size range which Lasue et al. (2009) used in their paper. They studied comet Halley and comet Hale-Bopp using a mixture of fluffy aggregates and compact solid grains and successfully explained the observed polarization characteristics of the two comets. In a follow-up paper, we also plan to model cometary dust as a mixture of aggregates and compact particles.

6 CONCLUSIONS

1. The size parameter of the monomer, $x \sim 1.56 - 1.70$, turned out to be the most suitable which provides the best fits to the observed polarization data of comet Hyakutake at three wavelengths: $\lambda = 0.365 \mu\text{m}$, $0.485 \mu\text{m}$ and $0.684 \mu\text{m}$. This corresponds to $0.090 \mu\text{m} \leq a_m \leq 0.098 \mu\text{m}$ at $\lambda = 0.365 \mu\text{m}$, $0.120 \mu\text{m} \leq a_m \leq 0.131 \mu\text{m}$ at $\lambda = 0.485 \mu\text{m}$ and $0.174 \mu\text{m} \leq a_m \leq 0.186 \mu\text{m}$ at $\lambda = 0.684 \mu\text{m}$.
2. The best fit refractive indices derived from the present analysis are $n = 1.745$ and $k = 0.095$ for $N = 128$ at $\lambda = 0.365 \mu\text{m}$; $n = 1.743$ and $k = 0.100$ for $N = 128$ at $\lambda = 0.485 \mu\text{m}$ and $n = 1.695$ and $k = 0.100$ for $N = 128$ at $\lambda = 0.684 \mu\text{m}$. These values resemble the mixture of silicates and carbonaceous compounds.
3. The negative polarization values have been successfully generated for $\theta > 157^\circ$ at three wavelengths.
4. We plan a follow-up paper where computations will be made considering a mixture of aggregates and compact spheroidal particles over a wide size range of the particles.

Acknowledgements The authors HSD and AKS acknowledge the Inter University Center for Astronomy and Astrophysics (IUCAA), Pune, for its associateship program. The authors acknowledge T. Mukai and Y. Okada for their help on the execution of BPCA and BCCA codes. The authors are thankful to D. Mackowski, K. Fuller, and M. Mishchenko, who made their superposition T-matrix code publicly available. The authors greatly acknowledge the referee for his valuable suggestions and comments which improved the quality of the paper.

References

- Bertini, I., Thomas, N., & Barberi, C. 2007, *A&A*, 461, 351
 Bockelée - Morvan, D., Gautier, D., Hersant, F., Huré, J. M., & Robert, F. 2002, *A&A*, 384, 1107
 Brownlee, D. E., Pilachowski, L., Olszewski, E., & Hodge, P. W. 1980, in *Solid Particles in the Solar System*, eds. I. Halliday, & B. A. McIntosh (Dordrecht: D. Reidel), 333
 Chernova, G. P., Kiselev, N. N., & Jockers, K. 1993, *Icarus*, 103, 144
 Das, H. S., Sen, A. K., & Kaul, C. L. 2004, *A&A*, 423, 373
 Das, H. S., & Sen, A. K. 2006, *A&A*, 459, 271
 Das, H. S., Das, S. R., Paul, T., Suklabaidya, A., & Sen, A. K. 2008a, *MNRAS*, 389, 787
 Das, H. S., Das, S. R., & Sen, A. K. 2008b, *MNRAS*, 390, 1195
 Dollfus, A. 1989, *A&A*, 213, 469
 Dorschner, J., Begemann, B., Henning, Th., Jäger, C., & Mutschke, H. 1995, *A&A*, 300, 503
 Fulle, M., Lévassieur-Regourd, A. C., McBride, N., & Hadamcik, E. 2000, *AJ*, 119, 1968
 Ganesh, S., Joshi, U. C., Baliyan, K. S., & Deshpande, M. R. 1998, *A&AS*, 129, 489
 Greenberg, J. M., & Hage, J. I. 1990, *ApJ*, 361, 260
 Gustafson, B. Å. S., & Kolokolova, L. 1999, *J. Geophys. Res.*, 104, 31711
 Hanner, M. S. 1999, *Space Sci. Rev.* 90, 99
 Hanner, M.S., & Bradley, J. P. 2004, *Comets II*, eds. M. C. Festou, H. U. Keller, & H. A. Weaver (Tucson, AZ: Univ. Arizona Press), 555

- Hadamcik, E., Renard, J. B., Worms, J. C., et al. 2002, *Icarus*, 155, 497
- Hadamcik, E., Renard, J. B., Levasseur-Regourd, A. C., & Lasue, J. 2006, *JQSRT*, 100, 143
- Harker, D. E., Woodward, C. E., Wooden, D. H., Witteborn, F. C., & Meyer, A. W. 1999, *AJ*, 118, 1423
- Harker, D. E., Wooden, D. H., Woodward, C. E., & Lisse, C. M. 2002, *ApJ*, 580, 579
- Hayward, T. L., Hanner, M. S., & Sekanina, Z. 2000, *ApJ*, 538, 428
- Hörz, F., Bastien, R., Borg, J., Bradley, J. P., Bridges, J. C., Brownlee, D. E., Burchell, M. J., Chi, M., et al. 2006, *Science*, 314, 1716
- Jessberger, E. K., Christoforidis, A., & Kissel, J. 1988, *Nature*, 332, 691
- Jessberger, E. K. 1999, *Space Sci. Rev.*, 90, 91
- Jewitt, D. 2004, *AJ*, 128, 3061
- Jockers, K., Kiselev, N., Bonev, T., et al. 2005, *A&A*, 441, 773
- Joshi, U. C., Baliyan, K. S., Ganesh, S., Chitre A., Vats, H. O., & Deshpande, M. R. 1997, *A&A*, 319, 694
- Kikuchi, S., Mikami, Y., Mukai, T., Mukai, S., & Hough, J. H. 1987, *A&A*, 187, 689
- Kimura, H. 2001, *JQSRT*, 70, 581
- Kimura, H., Kolokolova, L., & Mann, I. 2003, *A&A*, 407, L5
- Kimura, H., Kolokolova, L., & Mann, I. 2006, *A&A*, 449, 1243
- Kiselev, N. N., & Velichko, F. P. 1998, *Icarus*, 133, 286
- Kiselev, N. N., Jockers, K., Rosenbush, V. K., & Korsun, P. P. 2001, *Solar System Research*, 35, 480
- Kiselev, N. N., Jockers, K., & Bonev, T. 2004, *Icarus*, 168, 385
- Kissel, J., Sagdeev, R. Z., Bertaux, J. L., et al. 1986, *Nature*, 321, 280
- Kolokolova, L., Kimura, H., Ziegler, K., & Mann, I. 2006, *JQSRT*, 100, 199
- Kolokolova, L., Kimura, H., Kiselev, N., & Rosenbush, V. 2007, *A&A*, 463, 1189
- Lamy, P. L., Grün, E., & Perrin, J. M. 1987, *A&A*, 187, 767
- Lasue, J., & Levasseur-Regourd, A. C. 2006, *JQSRT*, 100, 220
- Lasue, J., Levasseur-Regourd, A. C., Hadamcik, E., & Alcouffe, G. 2009, *Icarus*, 199, 129
- Levasseur-Regourd, A. C., Hadamcik, E., & Renard, J. B. 1996, *A&A*, 313, 327
- Levasseur-Regourd, A. C. 1999, *Space Sc. Rev.*, 90, 163
- Levasseur-Regourd, A. C., & Hadamcik, E. 2003, *JQSRT*, 79, 911
- Levasseur-Regourd, A. C., Mukai, T., Lasue, J., & Okada, Y. 2007, *Planet. Space Sc.*, 55, 1010
- Levasseur-Regourd, A. C., Zolensky, M., & Lasue, J. 2008, *Planet. Space Sc.*, 56, 1719
- Lisse, C. M., A'Hearn, M. F., Hauser, M. G., Kelsall, T., Lien, D. J., Moseley, S. H., Reach, W. T., & Silverberg, R. F. 1998, *ApJ*, 496, 971
- Lisse, C. M. 2002, *Earth, Moon, and Planet*, 90, 497
- Mackowski, D. W., & Mishchenko, M. I. 1996, *J. Opt. Soc. Am. A*, 13, 2266
- Manset, N., & Bastien, P. 2000, *Icarus*, 145, 203
- Moreno, F., Munoz, O., Vilaplana, R., & Molina, A. 2003, *ApJ*, 595, 522
- Mukai, T., Ishimoto, H., Kozasa, T., Blum, J., & Greenberg, J. M. 1992, *A&A*, 262, 315
- Petrova, E. V., Tishkovets, V. P., & Jockers, K. 2004, *Solar System Res.*, 38, 309
- Sen, A. K., Deshpande, M. R., Joshi, U. C., Rao, N. K., & Raveendran, A. V. 1991a, *A&A*, 242, 496
- Sen, A. K., Joshi, U. C., & Deshpande, M. R. 1991b, *MNRAS*, 253, 738
- Shen, Y., Draine, B. T., & Johnson, E. T. 2009, *ApJ*, 696, 2126
- Sitko, M. L., Lynch, D. K., Russell, R. W., & Hanner, M. S. 2004, *ApJ*, 612, 576
- Tishkovets, V. P., Petrova, E. V., & Jockers, K. 2004, *JQSRT*, 86, 241
- Wurm, G., & Blum, J. 1998, *Icarus*, 132, 125
- Wooden, D. H., Harker, D. E., Woodward, C. E., et al. 1999, *ApJ*, 517, 1034
- Wooden, D. H., Butner, H. M., Harker, D. E., & Woodward, C. E. 2000, *Icarus*, 143, 126
- Xing, Z., & Hanner, M. S. 1997, *A&A*, 324, 805
- Zolensky, M. E., Zega, T. J., Yano, H., et al. 2006, *Science*, 314, 1735